Front. Phys. 12(5), 127502 (2017)
DOI 10.1007/s11467-017-0690-x

RESEARCH ARTICLE

Simulating heavy fermion physics in optical lattice: Periodic Anderson model with harmonic trapping potential

Yin Zhong[1,†], **Yu Liu**[2,3], **Hong-Gang Luo**[1,4]

[1] *Center for Interdisciplinary Studies & Key Laboratory for Magnetism and Magnetic Materials of the MoE, Lanzhou University, Lanzhou 730000, China*
[2] *LCP, Institute of Applied Physics and Computational Mathematics, Beijing 100088, China*
[3] *Software Center for High Performance Numerical Simulation, China Academy of Engineering Physics, Beijing 100088, China*
[4] *Beijing Computational Science Research Center, Beijing 100084, China*
Corresponding author. E-mail: [†] *zhongy05@hotmail.com*
Received October 26, 2016; accepted April 20, 2017

The periodic Anderson model (PAM), where local electron orbitals interplay with itinerant electronic carriers, plays an essential role in our understanding of heavy fermion materials. Motivated by recent proposals for simulating the Kondo lattice model (KLM) in terms of alkaline-earth metal atoms, we take another step toward the simulation of PAM, which includes the crucial charge/valence fluctuation of local f-electrons beyond purely low-energy spin fluctuation in the KLM. To realize PAM, a transition induced by a suitable laser between the electronic excited and ground state of alkaline-earth metal atoms ($^1S_0 \rightleftharpoons {}^3P_0$) is introduced. This leads to effective hybridization between local electrons and conduction electrons in PAM. Generally, the $SU(N)$ version of PAM can be realized by our proposal, which gives a unique opportunity to detect large-N physics without complexity in realistic materials. In the present work, high-temperature physical features of standard [$SU(2)$] PAM with harmonic trapping potential are analyzed by quantum Monte Carlo and dynamic mean-field theory, where the Mott/orbital-selective Mott state was found to coexist with metallic states. Indications for near-future experiments are provided. We expect our theoretical proposal and (hopefully) forthcoming experiments will deepen our understanding of heavy fermion systems. At the same time, we hope these will trigger further studies on related Mott physics, quantum criticality, and non-trivial topology in both the inhomogeneous and nonequilibrium realms.

Keywords optical lattice, heavy fermion, Mott transition

PACS numbers 75.30.Mb, 71.10.Fd, 37.10.Jk

1 Introduction

Understanding emergent novel collective quantum effects in heavy fermion systems, e.g., quantum criticality, strange metal, hidden order, and unconventional superconductivity [1–7], is one of most fundamental issues in modern condensed matter physics. In these materials, the electronic effective mass is significantly enhanced compared with normal metals. In addition, local f-electron orbits interplay with itinerant charge carriers, which is believed to be an essential driving force for those mentioned emergent phenomena [8]. However, in spite of decades of intensive theoretical and experimental research, the nature of these systems is still poorly understood, and even the most simplified models of Hamiltonian-like Kondo lattice (KLM) and periodic Anderson lattice (PAM) defy investigation owing to notorious fermion minus-sign problems [9, 10].

Fortunately, thanks to the rapid development of the ultracold fermionic atom loaded in an optical lattice [11–17], an intriguing plan to simulate a Kondo lattice model in terms of alkaline-earth metal atoms ^{87}Sr and ^{173}Yb

*arXiv: 1610.04372.

was recently proposed. Preliminary theoretical works in this direction have been published [18–26]. More recently, interactions in these alkaline-earth atom gases have been under control in terms of the newly proposed orbital Feshbach resonance [27–29]. (Although ^{173}Yb is in practice a rare-earth atom, it has an electronic structure similar to an alkaline-earth metal atom. We will use only the name "alkaline-earth metal atoms" for simplicity.) In realistic heavy fermion compounds, the charge/valence fluctuation of the local f-electron plays a crucial role in many mixed valence materials including the hotly studied candidate of *topological* Kondo insulator SmB_6 [30]. Furthermore, valance fluctuation is also argued to be responsible for the second superconducting phases in prototypical heavy fermion superconductors $CeCu_2Si_2$ and volume-changed transitions in monovalent Ce under high pressure [31, 32]. More theoretically, the orbital-selective Mott transition proposed for the heavy fermion quantum criticality is rooted in the localization of the f-electron driven by a large charge fluctuation, as well [33, 34].

Intrigued by those interesting phenomena, the periodic Anderson model (see also Fig. 1), which is a lattice extension of the well-known single impurity Anderson model and is believed to capture such charge/valence fluctuations in the simplest fashion, should be taken into account. However, to our knowledge, there are still no proposals to realize this fundamental model Hamiltonian in cold fermion systems.

In this article, we take the first step with regard to this issue by providing a simple scheme to realize a periodic Anderson model in alkaline-earth metal atoms, and to analyze the basic features of this model with state-of-the-art numeric tools: the numerically exact determinant quantum Monte Carlo (DQMC) supplemented with dynamic mean-field theory (DMFT) [35–38]. The latter one correctly captures local quantum many-body

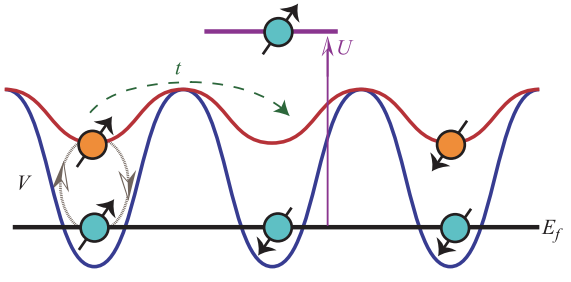

Fig. 1 The periodic Anderson model describes the hybridization V between a local electron orbital (*blue*) and a conducting charge carrier (*orange*). The single occupied local electron has energy E_f, while a double occupation has extra Coloumb energy U. The conduction electron hops t between nearest-neighbor sites, and it gives a conducting energy band. For simplicity, external harmonic trapping potential is not shown here.

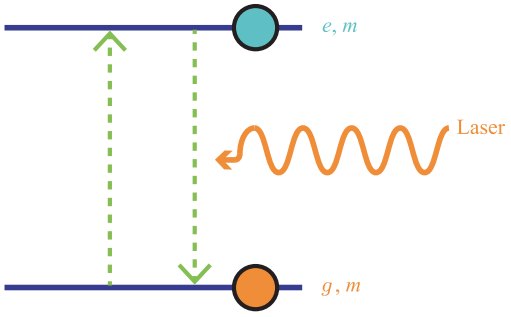

Fig. 2 An extra laser field is applied to induce a direct transition between the electronic excited (e, m) and ground (g, m) state, e.g., $^1S_0 \rightleftharpoons {}^3P_0$ (nuclear Zeeman state denoted by m is intact), which is able to simulate an effective hybridization V between a local electron and conduction electron in a periodic Anderson model. (For simplicity, only coupling with the same Zeeman sublevel is considered here.)

dynamics, and prediction becomes exact at an infinite dimension. The main point of the scheme is that the transition between an electronic excited state $^3P_0$ and ground state $^1S_0$ of alkaline-earth metal atoms such as ^{87}Sr and ^{173}Yb is driven by a suitably chosen laser field, which is used to give an effective $c-f$ hybridization between local electrons and conduction ones in PAM (See also Fig. 2). Here, the electronic excited state mimics the local f-electron, and the ground state represents the conduction electron but without a spin degree of freedom. Meanwhile, the nuclear Zeeman state, which is used to denote the effective/pseudo spin state in PAM, is intact. Combining these elements provides a potential scheme to simulate PAM with proper tuning of experimental parameters as proposed for KLM and as used in the fermionic Hubbard model [11, 12, 18, 19]. We should emphasize that in contrast to the usual PAM in condensed matter physics, because an external trapping potential always exists in an optical lattice system, PAM in a cold atom simulation must be supplemented with this (harmonic) trapping potential. Its simulation proposal and calculation are not reported in the existing literature but are achieved in this work.

Interestingly, the general $SU(N)$ version of PAM can be realized in our proposal. Although heavy fermion materials with an unfilled f-shell usually have a large degeneracy, and the widely used large-N expansion is controllable in this artificial limit [2], the complex chemical environment in realistic materials obscures the underlying physics, and the reliability of large-N theory is questioned. By contrast, the purity and tunability of an optical lattice system gives us a unique opportunity to directly detect the large-N physics of PAM and inspect what has been captured by our current theoretical understanding.

Furthermore, since a reachable temperature is compar-

atively high in the present ultracold atom field, numerical simulations of DQMC and DMFT can provide the basic physics for such a high-temperature regime, where Mott or orbital-selective Mott phenomena are clearly seen in the spatial-dependent density distribution and energy-sensitive density of the state. It is found that these Mott insulating states coexist with metallic states in real space, which should be seen in realistic experiments owing to their inevitable harmonic potential. These quantities can be measured by current cold-atom techniques. Future developments in alkaline-earth metal atoms are expected to realize the proposed PAM and to detect its intriguing nature of quantum many-body correlation. Moreover, if the standard PAM can be constructed, this may lead to a more exciting topological PAM involving subtle interplay between electron correlation and nontrivial band topology encoded by spin-orbital coupling. Given this, the idea of a topological Kondo insulator can be explored without its intrinsic complexity in realistic materials as SmB_6 [30].

The remainder of this paper is organized as follows. In Section 2, the proposal to realize PAM is analyzed, and a PAM Hamiltonian is derived from a general second quantized Hamiltonian for alkaline-earth metal atoms. In Section 3, high-temperature properties are discussed, and the Mott physics of the f-electron in harmonic trapping potential is explored. Finally, Section 4 is devoted to a brief discussion and conclusion.

2 Proposal to realize periodic Anderson model

The general second quantized Hamiltonian for alkaline-earth metal atoms reads

$$
\begin{aligned}
H=&H_G+H_{hy},\\
H_G=&\sum_{\alpha m}\int \mathrm{d}^3\boldsymbol{r}\Psi^\dagger_{\alpha m}(\boldsymbol{r})\left[-\frac{\hbar^2}{2M}\nabla^2+V_\alpha(\boldsymbol{r})\right]\Psi_{\alpha m}(\boldsymbol{r})\\
&+\hbar\omega_0\int \mathrm{d}^3\boldsymbol{r}[\rho_e(\boldsymbol{r})-\rho_g(\boldsymbol{r})]\\
&+\frac{g^+_{eg}+g^-_{eg}}{2}\int \mathrm{d}^3\boldsymbol{r}\rho_e(\boldsymbol{r})\rho_g(\boldsymbol{r})\\
&+\sum_{\alpha,m<m'}g_{\alpha\alpha}\int \mathrm{d}^3\boldsymbol{r}\rho_{\alpha m}(\boldsymbol{r})\rho_{\alpha m'}(\boldsymbol{r})\\
&+\frac{g^+_{eg}-g^-_{eg}}{2}\sum_{mm'}\int \mathrm{d}^3\boldsymbol{r}\Psi^\dagger_{gm}(\boldsymbol{r})\Psi^\dagger_{em'}(\boldsymbol{r})\Psi_{gm'}(\boldsymbol{r})\Psi_{em}(\boldsymbol{r}),\\
H_{hy}=&g_l\sum_m\int \mathrm{d}^3\boldsymbol{r}[\Psi^\dagger_{em}(\boldsymbol{r})\Psi_{gm}(\boldsymbol{r})+\Psi^\dagger_{gm}(\boldsymbol{r})\Psi_{em}(\boldsymbol{r})],
\end{aligned}
\tag{1}
$$

where fermion field operator $\Psi^\dagger_{\alpha m}(\boldsymbol{r})$ creates an atom at position $\boldsymbol{r}$ with internal state $|\alpha m\rangle$, $\rho_{\alpha m}=\Psi^\dagger_{\alpha m}(\boldsymbol{r})\Psi_{\alpha m}(\boldsymbol{r})$ and $\rho_\alpha=\sum_{m=-I}^{I}\rho_{\alpha m}$. Here, $\alpha=g$ or e denotes an electronic state $^1S_0$ (ground state) and $^3P_0$ (excited state), respectively. Furthermore, the nuclear Zeeman states of alkaline-earth metal atoms are represented by $m=-I,-I+1,\ldots,I-1,I$. For example, ^{87}Sr has $I=9/2$, ^{171}Yb has $I=1/2$, and ^{173}Yb has $I=5/2$. The external potential $V_\alpha(\boldsymbol{r})$ is provided by the optical lattice, and both periodic potential and harmonic trapping potential are included. The energy shift of the excited state to the ground state is $\hbar\omega_0$ and $g_{gg}, g_{ee}, g^+_{eg}, g^-_{eg}$m which are all interaction parameters. However, because the alkaline-earth metal atoms have a fully occupied outer shell and their total electron spin is zero, the conventional magnetic Feshbach resonance cannot tune the interaction between two atoms. Fortunately, the newly proposed orbital Feshbach resonance can tune the interaction in these alkaline-earth atom systems. This has been realized for the ^{173}Yb atom gas [27–29].

We should point out that H_G was introduced by Gorshkov *et al.* to describe a scheme for the simulation of a Kondo lattice model [18]. The extra Hamiltonian H_{hy} is added in the present work but is not covered in their original proposal. This extra term with a coupling constant g_l expresses a transition between the excited and ground state (e.g., $^1S_0 \rightleftharpoons {}^3P_0$) of alkaline-earth metal atoms such as ^{87}Sr and ^{173}Yb, which can be induced by an extra laser field [39, 40]. Here, generically, the coupling of a different nuclear Zeeman sublevel as $\sum_{m,m'} g_l^{m,m'}\int \mathrm{d}^3\boldsymbol{r}[\Psi^\dagger_{em}(\boldsymbol{r})\Psi_{gm'}(\boldsymbol{r})+\Psi^\dagger_{gm'}(\boldsymbol{r})\Psi_{em}(\boldsymbol{r})]$ is possible, but we choose the simplest case $g_l^{m,m'}=g_l\delta_{m,m'}$ with a suitable driving laser frequency and polarization. In the following discussion, we can see that this extra term will lead to the realization of a periodic Anderson model since effective c–f hybridization is induced by this direct transition. Before leaving this issue, we note that if nearest-neighbor c–f hybridization with spin dependence can be realized, one expects that the topological periodic Anderson model can be explored [41], and the physics of the advocated topological Kondo insulator may be inspected from this alternative point of view apart from real-life material SmB_6.

Then, assuming only the lowest energy band is involved in our model, we expand

$$\Psi_{gm}(\boldsymbol{r})=\sum_j w_g(\boldsymbol{r}-\boldsymbol{r}_j)c_{jm}, \tag{2}$$

$$\Psi_{em}(\boldsymbol{r})=\sum_j w_e(\boldsymbol{r}-\boldsymbol{r}_j)f_{jm}, \tag{3}$$

where a real Wannier function $w_\alpha(\boldsymbol{r})$ is utilized, and c_{jm} (f_{jm}) destroys an atom-located site j with internal state $|gm\rangle$ ($|em\rangle$). Inserting these equations into Eq. (1) leads

to a lattice Hamiltonian as follows:

$$\begin{aligned}H=&-t_c\sum_{\langle ij\rangle m}c^\dagger_{im}c_{jm}-t_f\sum_{\langle ij\rangle m}f^\dagger_{im}f_{jm}\\&-\mu_c\sum_{jm}c^\dagger_{jm}c_{jm}-\mu_f\sum_{jm}f^\dagger_{jm}f_{jm}\\&+U_c\sum_{j,m<m'}c^\dagger_{jm}c_{jm}c^\dagger_{jm'}c_{jm'}\\&+U_f\sum_{j,m<m'}f^\dagger_{jm}f_{jm}f^\dagger_{jm'}f_{jm'}\\&+U_{cf}\sum_{j,m,m'}c^\dagger_{jm}c_{jm}f^\dagger_{jm'}f_{jm'}\\&+U_{ex}\sum_{j,m,m'}c^\dagger_{jm}f^\dagger_{jm'}c_{jm'}f_{jm}\\&+V\sum_{j,m}(c^\dagger_{jm}f_{jm}+f^\dagger_{jm}c_{jm}).\end{aligned}\tag{4}$$

Here, as is often done in simulations of the fermionic Hubbard model [42], only nearest-neighbor hopping is considered, and the harmonic trapping potential is not explicitly considered but will be added later. Furthermore, a single center approximation is made, which means only interactions at the same site are considered $U^\phi_{ijkl}=U_\phi\delta_{i=j=k=l}$ with $\phi=c,f,cf,ex$.

The parameters in the lattice model are related to the original Hamiltonian via

$$\begin{aligned}t_c&=-\int \mathrm{d}^3\boldsymbol{r}w_g(\boldsymbol{r})\left[-\frac{\hbar^2}{2M}\nabla^2+V_g(\boldsymbol{r})\right]w_g(\boldsymbol{r}+\boldsymbol{\delta}),\\t_f&=-\int \mathrm{d}^3\boldsymbol{r}w_e(\boldsymbol{r})\left[-\frac{\hbar^2}{2M}\nabla^2+V_e(\boldsymbol{r})\right]w_e(\boldsymbol{r}+\boldsymbol{\delta}),\\\mu_c&=-\int \mathrm{d}^3\boldsymbol{r}w_g(\boldsymbol{r})\left[-\frac{\hbar^2}{2M}\nabla^2+V_g(\boldsymbol{r})+\hbar\omega_0\right]w_g(\boldsymbol{r}),\\\mu_f&=-\int \mathrm{d}^3\boldsymbol{r}w_e(\boldsymbol{r})\left[-\frac{\hbar^2}{2M}\nabla^2+V_e(\boldsymbol{r})-\hbar\omega_0\right]w_e(\boldsymbol{r}),\\U_c&=g_{gg}\int \mathrm{d}^3\boldsymbol{r}w_g^4(\boldsymbol{r}),\\U_f&=g_{ee}\int \mathrm{d}^3\boldsymbol{r}w_e^4(\boldsymbol{r}),\\U_{cf}&=\frac{g^+_{eg}+g^-_{eg}}{2}\int \mathrm{d}^3\boldsymbol{r}w_g^2(\boldsymbol{r})w_e^2(\boldsymbol{r}),\\U_{ex}&=\frac{g^+_{eg}-g^-_{eg}}{2}\int \mathrm{d}^3\boldsymbol{r}w_g^2(\boldsymbol{r})w_e^2(\boldsymbol{r}),\\V&=g_l\int \mathrm{d}^3\boldsymbol{r}w_g(\boldsymbol{r})w_e(\boldsymbol{r}),\end{aligned}\tag{5}$$

where nearest-neighbor vector $\boldsymbol{\delta}$ is defined.

Now, if we adjust $g^+_{eg}=g^-_{eg}$ via a suitable Feshbach resonance technique, the spin-spin exchange interaction U_{ex}, which is responsible for the simulation of the Kondo lattice model, vanishes in this case. Next, the local interaction U_c and hopping t_f can also be tuned to be small, and are thus neglected. The resulting Hamiltonian reads

$$\begin{aligned}H=&-t_c\sum_{\langle ij\rangle m}c^\dagger_{im}c_{jm}-\mu_c\sum_{jm}c^\dagger_{jm}c_{jm}-\mu_f\sum_{jm}f^\dagger_{jm}f_{jm}\\&+U_f\sum_{j,m<m'}f^\dagger_{jm}f_{jm}f^\dagger_{jm'}f_{jm'}\\&+U_{cf}\sum_{j,m,m'}c^\dagger_{jm}c_{jm}f^\dagger_{jm'}f_{jm'}\\&+V\sum_{j,m}(c^\dagger_{jm}f_{jm}+f^\dagger_{jm}c_{jm}).\end{aligned}\tag{6}$$

After rescaling the hopping and chemical potential parameters as $t_c\to t$, $\mu_c\to\mu$, $-\mu_f\to E_f$ and re-explaining the fermion operator c_{jm} (f_{jm}) as an annihilation operator for the conduction electron (local f-electron) with internal "spin" state m, we arrive at the so-called $SU(N)$ periodic Anderson model with spin degeneracy $N=2I+1$ [2]:

$$\begin{aligned}H_{SU(N)}=&-t\sum_{\langle ij\rangle m}c^\dagger_{im}c_{jm}-\mu\sum_{jm}c^\dagger_{jm}c_{jm}\\&+E_f\sum_{jm}f^\dagger_{jm}f_{jm}+V\sum_{j,m}(c^\dagger_{jm}f_{jm}+f^\dagger_{jm}c_{jm})\\&+U_f\sum_{j,m<m'}f^\dagger_{jm}f_{jm}f^\dagger_{jm'}f_{jm'}\\&+U_{cf}\sum_{j,m,m'}c^\dagger_{jm}c_{jm}f^\dagger_{jm'}f_{jm'}.\end{aligned}\tag{7}$$

Currently, the above $SU(N)$ model may be realized for cases with $N=2,6,10$, which corresponds to ^{171}Yb, ^{173}Yb and ^{87}Sr atom gases. Although the heavy fermion materials with unfilled f-shells usually have such a large degeneracy, the complex chemical environment in realistic materials obscures the underlying physics. Moreover, large-N expansion is widely utilized in the heavy fermion community, but the reliability of this theoretical tool is not clear as compared with experiments owing to the mentioned complication [2]. By contrast, the purity and tunability of an optical lattice system gives us a unique opportunity to directly detect the large-N physics of PAM.

Furthermore, if we are interested in the case with $N=2$, where only two nuclear Zeeman sublevels are considered, the more familiar $SU(2)$ version is obtained:

$$\begin{aligned}H_{SU(2)}=&-t\sum_{\langle ij\rangle\sigma}c^\dagger_{i\sigma}c_{j\sigma}-\mu\sum_{j\sigma}c^\dagger_{j\sigma}c_{j\sigma}+E_f\sum_{j\sigma}f^\dagger_{j\sigma}f_{j\sigma}\\&+V\sum_{j\sigma}(c^\dagger_{j\sigma}f_{j\sigma}+f^\dagger_{j\sigma}c_{j\sigma})+U\sum_j n^f_{j\uparrow}n^f_{j\downarrow}\\&+U_{cf}\sum_j n^c_j n^f_j\end{aligned}\tag{8}$$

with effective electronic spin $\sigma=\uparrow,\downarrow$, $U_f\to U$, $n_{j\sigma}=f^\dagger_{j\sigma}f_{j\sigma}$ and $n^f_j=\sum_\sigma n_{j\sigma}$. Finally, a simplification can

be made when U_{cf} is small compared with other energy scales, and the system is far away from an f-electron valence transition. Then, the standard PAM reads

$$H_{\rm PAM} = -t\sum_{\langle ij\rangle\sigma} c^\dagger_{i\sigma}c_{j\sigma} - \mu\sum_{j\sigma} c^\dagger_{j\sigma}c_{j\sigma} + E_f\sum_{j\sigma} f^\dagger_{j\sigma}f_{j\sigma} + V\sum_{j\sigma}(c^\dagger_{j\sigma}f_{j\sigma} + f^\dagger_{j\sigma}c_{j\sigma}) + U\sum_j n^f_{j\uparrow}n^f_{j\downarrow}. \quad (9)$$

Because the alkaline(rare)-earth metal atom ^{171}Yb has nuclear spin $I = 1/2$, it has the potential to realize the $SU(2)$ PAM in terms of this ultracold atom gas.

Thus far, we have not specified the lattice structure onto which those ultracold atom gases are loaded. Generally, the one-dimensional chain, non-frustrated square, cubic and honeycomb lattices, and frustrated triangular and Kagome lattices have been realized in optical lattice systems [43]. The discussion below will focus on a one-dimensional chain and two-dimensional square lattice to give a physically transparent explanation of the underlying physics. Other more complex lattices are straightforward to explore but are not shown in the present work [44].

3 Basic features at high temperature

The discussion of generic properties of PAM in Eqs. (7)–(9) can be found in Refs. [1–3], and the interested reader may examine these references. Note, however, that in these references, no harmonic potential is considered, which is a crucial element of real-life optical lattices.

In current experiments of ultracold atoms in optical lattices, particularly for the realized fermionic Hubbard model, the achieved lowest effective temperature is about $T \sim t$ [13–15]. Although both the previously discussed Kondo lattice and our proposed periodic Anderson model have not been realized for alkaline-earth metal atoms, we expect near-future experiments in this direction may reach a similar temperature regime $T \sim t$.

Actually, for $T \geq t$, the system works in a relatively high temperature regime since the typical low-energy spin interaction scale, namely Kondo exchange coupling $J_K \simeq \frac{V^2}{U}$, is usually smaller than t for intermediate or large U ($U \geq 4t$, $U \gg V$). (The heavy fermion compounds have large U compared to its bandwidth). This means $T \geq J_K$. Thus, the corresponding Kondo physics ($T_K \sim te^{-t/J_K}$) or, more explicitly, the lattice Kondo effect, cannot be captured in our case. At the same time, the competitor of Kondo screening, the long-ranged RKKY magnetic interaction ($T_{\rm RKKY} \sim J_K^2/t < T$), is also out of the detectable high-temperature regime.

Although the mentioned low-temperature physics is beyond our reach, we can still observe many interesting phenomena in the high-temperature regime, which is able to be detected by current cold-atom techniques. For a realistic cold atom system, the external trapping potential, which is usually approximated as a harmonic potential to confine atoms, should be added to the models and may be simply considered as a site-dependent chemical potential as [42]

$$H_{\rm PAM} = -t\sum_{\langle ij\rangle\sigma} c^\dagger_{i\sigma}c_{j\sigma} + \sum_{j\sigma}\left[\frac{1}{2}\omega^2(r_j - r_0)^2 - \mu\right]c^\dagger_{j\sigma}c_{j\sigma} + \sum_{j\sigma}\left[\frac{1}{2}\omega^2(r_j - r_0)^2 + E_f\right]f^\dagger_{j\sigma}f_{j\sigma} + V\sum_{j\sigma}(c^\dagger_{j\sigma}f_{j\sigma} + f^\dagger_{j\sigma}c_{j\sigma}) + U\sum_j n^f_{j\uparrow}n^f_{j\downarrow}. \quad (10)$$

Here, for simplicity, we used the standard PAM, but the more involved $SU(N)$ version is readily obtained. The harmonic trapping potential is now represented as $\frac{1}{2}\omega^2(r_j - r_0)^2$ with the central site as r_0. The possible anisotropy of this harmonic potential is neglected because no qualitative changes appear [14].

As studied in the Hubbard model with harmonic potential, Mott physics without magnetism can be clearly seen in this system since charge excitation dominates when $T \geq t$ [14, 15, 45–47]. For PAM with a trapping potential such as that in Eq. (10), based on our deep understanding of uniform cases without external potential [33, 34, 48, 49], we expect an orbital-selective Mott transition to emerge where Mott localization develops only for the f-electron while the conduction electron is intact. If one detects only an f-electron, this may be treated as Mott physics for the f-electron. In the remaining part of this paper, we use Mott instead of the more correct name orbital-selective Mott by keeping this tiny difference in mind.

3.1 Density distribution and DQMC

The above expectation is verified by our DQMC calculation in Figs. 3 and 4, The occupation of the f-electron in real space is plotted, and a Mott regime with $n_f = \langle n_f\rangle \simeq 1$ is clearly seen in the central region. The metallic region occupies the edge part of the system. (Statistical errors are very small, on the order of 0.1 percent or less for all quantities considered, and are not shown.) Thus, the coexistence of the Mott and metal phases was observed. This is a generic feature of a strongly correlated system with regard to trapping potential [42]. Meanwhile, in Fig. 3, we also show the variance of the f-electron number at each site $\Delta n_f = \langle n_f^2\rangle - \langle n_f\rangle^2$. This behavior agrees with the results from inspecting the occupation number of f-electron n_f, where the charge fluctuation is heavily suppressed for the central Mott regime ($\Delta n_f \sim 0$), while a large variance indicates metallic behavior around the edge parts. It is noted that even in

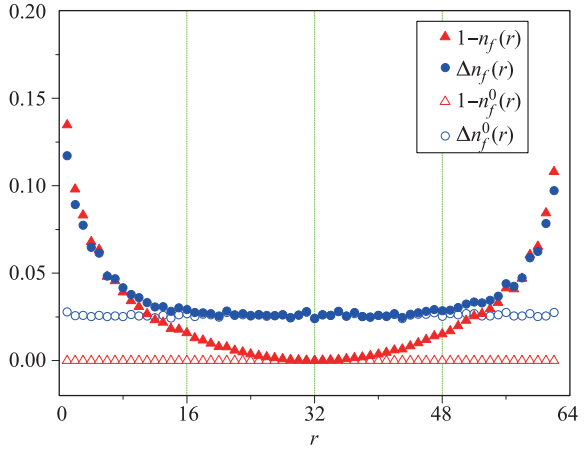

Fig. 3 f-electron real space density $n_f(r)$ and variance $\Delta n_f(r)$ distribution for 1D periodic Anderson model with harmonic potential. Calculation is performed for a 64-site system with open boundary condition and parameters $t = 1$, $V = 1$, $U = 12$, $E_f = -6$, $\mu = 0$, $\omega = 0.1$, $\Delta\tau = 0.0625$ and $T = 1$. The uniform case with $\omega = 0$ is also shown as $n_f^0(r)$ and $\Delta n_f^0(r)$.

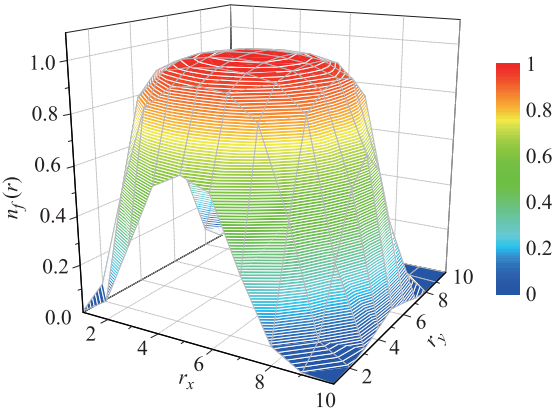

Fig. 4 f-electron real space density distribution for 2D periodic Anderson model with harmonic potential. A 10×10 square lattice system with open boundary condition is considered with parameters $t = 1$, $V = 1$, $U = 10$, $E_f = -5$, $\mu = 0$, $\omega = 0.8$, $\Delta\tau = 0.125$ and $T = 1$.

the Mott regime, the variance in the f-electron number Δn_f does not vanish since only when U is infinite is the charge fluctuation completely suppressed and gives $\Delta n_f = 0$. However, for systems with finite U that are located in a Mott insulating state, the charge fluctuation still survives, and a small but finite Δn_f is expected. In our case, we observe $\Delta n_f \simeq 0.025$ in the central Mott regime.

For a 2D system such as a square lattice as studied in Fig. 4, to have a sensible central Mott regime of about 20 sites, a large harmonic potential frequency $\omega = 0.8$ is chosen in contrast to the 1D chain case with $\omega = 0.1$, where most of the sites are single-occupied and show Mott insulating behavior. Obviously, if the harmonic potential is turned off, the Mott state exists only in such an unform background since the system is half-filled with the present parameters. These can be seen by inspecting n_f^0 and $\Delta n_f^0(r)$, e.g., in Fig. 3 for a 1D case. Additionally, we checked that small but finite harmonic potential affects only the boundary sites, while the inner sites show Mott localization as expected. (The density distribution of the conduction electron is shown in Fig. 5.) We note that site-resolved imaging of particle density distribution in a fermionic Mott insulator was recently achieved for ^{6}Li and ^{40}K [14, 15], and our calculated spatial distribution of electrons may be a good guide for the realization of PAM in terms of alkaline-earth metal atom gases.

Before ending this subsection, we remind the reader that the PAM with harmonic potential in fact has a severe fermion minus-sign problem for DQMC. For example, for a 10×10 square-lattice PAM with parameters in Fig. 4, the sign average is smaller than 0.1 when $T < t/2$. For a larger 12×12 system, even $T = t$ leads to a small sign average. Thus, we cannot obtain reliable low-temperature information, and the interesting Kondo or magnetic effect is out of reach.

3.2 Local density of state and DMFT

Additionally, the Mott behavior of the f-electron can be seen in their local density of state (DOS) where a large quasi-particle gap (or Mott gap) develops when the Mott localization of the f-electron is formed. In experiments, the mentioned Mott gap can be directly probed by measuring the response of the ultracold atom gas in the optical lattice to a modulation of the lattice depth in spite of the intrinsic spatial inhomogeneity induced by the harmonic trapping potential [12]. It is noted that this technique was successfully applied in the simulation of a fermionic Hubbard model with ^{40}K atoms [12]. Thus, we expect similar techniques may extract information about the Mott gap for alkaline-earth metal atoms ^{87}Sr and ^{173}Yb in a periodic Anderson model regime.

Here, owing to an elusive numerical analytic continuation by transforming imaginary-time quantum Monte Carlo data into real frequencies, and the severe fermion minus-sign problem for larger system sizes, we do not use DQMC to obtain an f-electron DOS . Instead, the dynamic mean-field theory (DMFT) approximation is the method of choice. For technical consideration, the harmonic external potential is turned off, and the corresponding f-electron DOS for a uniform system is shown in Fig. 6, which may still be helpful for understanding inhomogeneous cases since in experiment (Ref. [12]) performed on an inhomogeneous system, one finds a similar result as predicted by theory in a uniform lattice

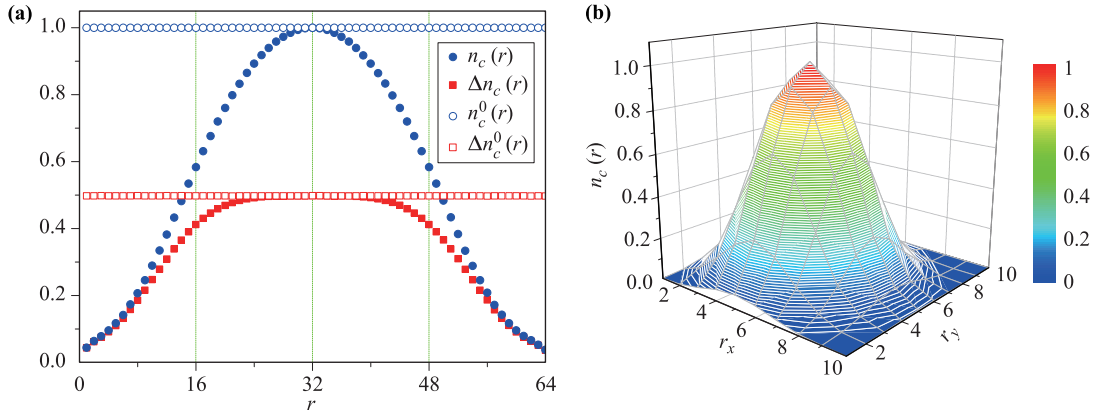

Fig. 5 **(a)** Conduction electron density distribution ($n_c(r)$, $n_c^0(r)$) for 1D PAM with harmonic potential $\omega = 0.1, 0$ and **(b)** 2D model with $\omega = 0.8$. Other parameters are identical to corresponding cases in Fig. 3 and Fig. 4.

model. In addition, thermometry, which means to find the effective equilibrium temperature or entropy per particle for experimental samples, is actually done by fitting measured data to theoretical results in a uniform model Hamiltonian [13, 50].

In Fig. 6, in order to have a Mott transition and the related Mott insulating state for the f-electron, a half-filled paramagnetic system is considered, and a fast solver called the iterated perturbation theory is used. This is able to obtain qualitative or semi-quantitative prediction compared with more exact but time-consuming solvers, at least for a half-filled system [38, 51]. From the calculation of DMFT, we see that a clear excitation gap is established between two broad bands (the so-called upper and lower Hubbard bands) when U is large ($U \gtrsim 12$). This means the Mott state for local f-electron is formed via a large Hubbard U to prohibit double occupation on each site. As noted previously, this gap can be measured by corresponding techniques, and it also can be used to detect the formation of Hubbard bands. For comparison, the conduction electron DOS $D_c(\omega)$ is also shown. It is clear that no qualitative changes appear for the conduction electron during the Mott localization of the f-electron [52].

4 Conclusion and discussion

We have proposed a possible way to realize both a $SU(N)$ periodic Anderson model and its standard version, where universal heavy fermion physics in the condensed matter community is able to be detected and clarified by a well-developed optical lattice and cold-atom techniques. For $SU(2)$ PAM, the underlying high

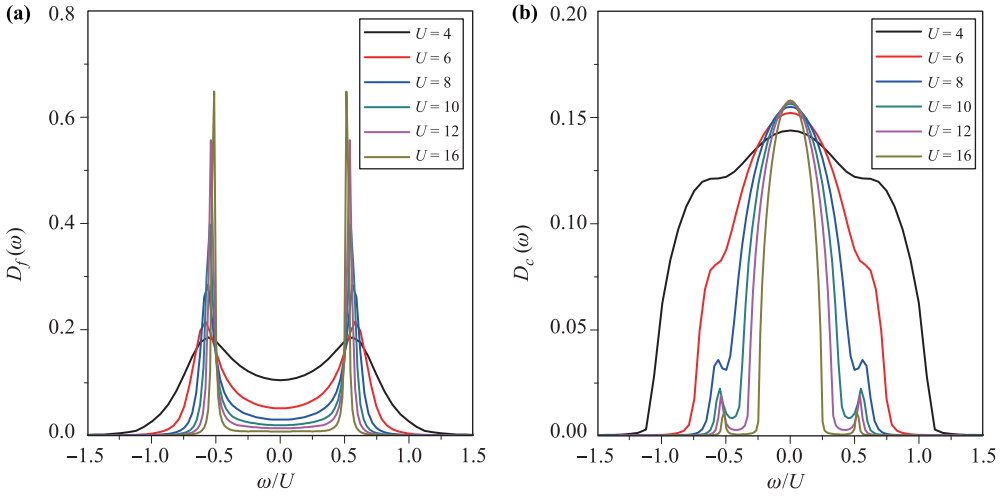

Fig. 6 **(a)** f-electron density of state $D_f(\omega)$ for 2D periodic Anderson model on square lattice with parameters $t = 1$, $V = 1$, $U = 4, 6, 8, 10, 12, 16$, $E_f = -U/2$ and $T = 1$. For comparison, the conduction electron density of state $D_c(\omega)$ is also shown **(b)**.

temperature but still interesting physics is explored by numerical simulations, i.e., DQMC and DMFT, where the spatial distribution of f-electron density and its local density of state are consistent with the expectation of Mott or orbital-selective Mott physics. These clear signatures of interaction-induced (orbital-selective) Mott localization states for local f-electrons may be helpful for corresponding experiments in this direction. Additionally, the $SU(N)$ physics of PAM have not been explored, but we expect novel physics beyond Doniach's classic phase diagram of a heavy fermion like charge-density-wave, valence-bond-solid and η-pairing should emerge as inspired by a corresponding large symmetry study of $SU(2N)$ Hubbard-like models [53–56].

Future investigations of detailed spin/charges or even pairing correlations at site scale are desirable because similar measurements have been performed with a fermionic Hubbard model [13, 16, 17]. In addition, if the effective temperature of an optical lattice can be further lowered, it will be interesting to study the low-energy/temperature-lattice Kondo physics and the corresponding two-fluid behavior [7], which is proposed as a core actor for almost all low-temperature anomalous quantum phenomena.

Another interesting issue is to explore the negative-U periodic Anderson model in these ultracold fermion systems. (Such negative-U can be tuned by the orbital Feshbeach resonance technique [27–29].) Such a negative U model can be (numerically) solved by DQMC, and has been argued as a phenomenological Hamiltonian for heavy fermion superconductivity [57]. Future work in this direction is helpful to uncover the nature of this effective model, and will be a good starting point for understanding the unconventional pairing mechanisms in those strongly correlated electron systems [58–61].

Note added in proof. After the completion of this work, Nakagawa and Kawakami brought their work to us [62], where they proposed a laser-induced PAM with spin-dependent $c-f$ hybridization, which is not the standard PAM proposed by us. Moreover, the $SU(N)$ physics is lost in their model and is distinct to ours.

Acknowledgements We thank Congjun Wu for helpful discussion on $SU(N)$ physics, and Ren Zhang for discussions about orbital Feshbach Resonance. This research was supported in part by the National Natural Science Foundation of China under Grant Nos. 11325417, 11674139, and 11504061, the China Postdoctoral Science Foundation, and the Foundation of LCP.

References

1. A. C. Hewson, The Kondo Problem to Heavy Fermions, Cambridge University Press, 1993
2. P. Coleman, Introduction to Many Body Physics, chapters 15 to 18, Cambridge University Press, 2015
3. H. Tsunetsugu, M. Sigrist, and K. Ueda, The ground-state phase diagram of the one-dimensional Kondo lattice model, *Rev. Mod. Phys.* 69(3), 809 (1997)
4. H. V. Löhneysen, A. Rosch, M. Vojta, and P. W¨olfle, Fermi-liquid instabilities at magnetic quantum phase transitions, *Rev. Mod. Phys.* 79(3), 1015 (2007)
5. C. Pfleiderer, Superconducting phases of f-electron compounds, *Rev. Mod. Phys.* 81(4), 1551 (2009)
6. J. A. Mydosh and P. M. Oppeneer, Hidden order, superconductivity, and magnetism: The unsolved case of URu_2 Si_2, *Rev. Mod. Phys.* 83(4), 1301 (2011)
7. Y. F. Yang, Two-fluid model for heavy electron physics, *Rep. Prog. Phys.* 79(7), 074501 (2016)
8. S. Doniach, The Kondo lattice and weak antiferromagnetism, *Physica B + C* 91, 231 (1977)
9. M. Vekić, J. W. Cannon, D. J. Scalapino, R. T. Scalettar, and R. L. Sugar, Competition between antiferromagnetic order and spin-liquid behavior in the two-dimensional periodic Anderson model at half filling, *Phys. Rev. Lett.* 74(12), 2367 (1995)
10. F. F. Assaad, Quantum Monte Carlo simulations of the half-filled two-dimensional Kondo lattice model, *Phys. Rev. Lett.* 83(4), 796 (1999)
11. M. Köhl, H. Moritz, T. Stöferle, K. Günter, and T. Esslinger, Fermionic atoms in a three dimensional optical lattice: Observing Fermi surfaces, dynamics, and interactions, *Phys. Rev. Lett.* 94(8), 080403 (2005)
12. R. Jördens, N. Strohmaier, K. Günter, H. Moritz, and T. Esslinger, A Mott insulator of fermionic atoms in an optical lattice, *Nature* 455(7210), 204 (2008)
13. R. A. Hart, P. M. Duarte, T. L. Yang, X. Liu, T. Paiva, E. Khatami, R. T. Scalettar, N. Trivedi, D. A. Huse, and R. G. Hulet, Observation of antiferromagnetic correlations in the Hubbard model with ultracold atoms, *Nature* 519(7542), 211 (2015)
14. D. Greif, M. F. Parsons, A. Mazurenko, C. S. Chiu, S. Blatt, F. Huber, G. Ji, and M. Greiner, Site-resolved imaging of a fermionic Mott insulator, *Science* 351(6276), 953 (2016)
15. L. W. Cheuk, M. A. Nichols, K. R. Lawrence, M. Okan, H. Zhang, and M. W. Zwierlein, Observation of 2D fermionic Mott insulators of K^{40} with single-site resolution, *Phys. Rev. Lett.* 116(23), 235301 (2016)
16. M. F. Parsons, A. Mazurenko, C. S. Chiu, G. Ji, D. Greif, and M. Greiner, Site-resolved measurement of the spin-correlation function in the Hubbard model, *Science* 353, 1253 (2016)
17. M. Boll, T. A. Hilker, G. Salomon, A. Omran, I. Bloch, and C. Gross, Spin and charge resolved quantum gas microscopy of antiferromagnetic order in Hubbard chains, *Science* 353, 1257 (2016)

18. A. V. Gorshkov, M. Hermele, V. Gurarie, C. Xu, P. S. Julienne, J. Ye, P. Zoller, E. Demler, M. D. Lukin, and A. M. Rey, Two-orbital $SU(N)$ magnetism with ultracold alkaline-earth atoms, *Nat. Phys.* 6(4), 289 (2010)
19. M. Foss-Feig, M. Hermele, and A. M. Rey, Probing the Kondo lattice model with alkaline-earth-metal atoms, *Phys. Rev. A* 81, 051603(R) (2010)
20. M. Foss-Feig, M. Hermele, V. Gurarie, and A. M. Rey, Heavy fermions in an optical lattice, *Phys. Rev. A* 82(5), 053624 (2010)
21. J. Silva-Valencia and A. M. C. Souza, Entanglement of alkaline-earth-metal fermionic atoms confined in optical lattices, *Phys. Rev. A* 85(3), 033612 (2012)
22. J. Silva-Valencia and A. M. C. Souza, Ground state of alkaline-earth fermionic atoms in one-dimensional optical lattices, *Eur. Phys. J. B* 85, 5 (2012)
23. B. N. Jiang, J. Qian, W. L. Wang, J. Du, and Y. Z. Wang, Interacting heavy fermions in a disordered optical lattice, *Eur. Phys. J. D* 68(12), 361 (2014)
24. L. Isaev and A. M. Rey, Heavy-fermion valence-bond liquids in ultracold atoms: Cooperation of the Kondo effect and geometric frustration, *Phys. Rev. Lett.* 115(16), 165302 (2015)
25. L. Isaev, J. Schachenmayer, and A. M. Rey, Spin-Orbit-coupled correlated metal phase in Kondo lattices: An implementation with alkaline-earth atoms, *Phys. Rev. Lett.* 117(13), 135302 (2016)
26. R. Zhang, D. P. Zhang, Y. T. Cheng, W. Chen, P. Zhang, and H. Zhai, Kondo effect in alkaline-earth-metal atomic gases with confinement-induced resonances, *Phys. Rev. A* 93(4), 043601 (2016)
27. R. Zhang, Y. T. Cheng, H. Zhai, and P. Zhang, Orbital Feshbach resonance in alkali-earth atoms, *Phys. Rev. Lett.* 115(13), 135301 (2015)
28. G. Pagano, M. Mancini, G. Cappellini, L. Livi, C. Sias, J. Catani, M. Inguscio, and L. Fallani, Strongly interacting gas of two-electron fermions at an orbital Feshbach resonance, *Phys. Rev. Lett.* 115(26), 265301 (2015)
29. M. Höfer, L. Riegger, F. Scazza, C. Hofrichter, D. R. Fernandes, M. M. Parish, J. Levinsen, I. Bloch, and S. Fölling, Observation of an orbital interaction-induced Feshbach resonance in Yb^{173}, *Phys. Rev. Lett.* 115(26), 265302 (2015)
30. M. Dzero, J. Xia, V. Galitski, and P. Coleman, Topological Kondo insulators, *Annu. Rev. Condens. Matter Phys.* 7(1), 249 (2016)
31. H. Q. Yuan, F. M. Grosche, M. Deppe, C. Geibel, G. Sparn, and F. Steglich, Observation of two distinct superconducting phases in $CeCu_2Si_2$, *Science* 302(5653), 2104 (2003)
32. J. P. Rueff, J. P. Itie, M. Taguchi, C. F. Hague, J. M. Mariot, R. Delaunay, J. P. Kappler, and N. Jaouen, Probing the $\gamma-\alpha$ transition in bulk Ce under pressure: A Direct investigation by resonant inelastic X-ray scattering, *Phys. Rev. Lett.* 96(23), 237403 (2006)
33. C. Pépin, Kondo breakdown as a selective Mott transition in the Anderson lattice, *Phys. Rev. Lett.* 98(20), 206401 (2007)
34. Y. Zhong, K. Liu, Y. Q. Wang, and H. G. Luo, Alternative Kondo breakdown mechanism: Orbital-selective orthogonal metal transition, *Phys. Rev. B* 86(11), 115113 (2012)
35. R. Blankenbecler, D. J. Scalapino, and R. L. Sugar, Monte Carlo calculations of coupled boson-fermion systems (I), *Phys. Rev. D* 24(8), 2278 (1981)
36. J. E. Hirsch, Two-dimensional Hubbard model: Numerical simulation study, *Phys. Rev. B* 31(7), 4403 (1985)
37. R. R. dos Santo, *Braz. J. Phys.* 33, 1 (2003)
38. A. Georges, G. Kotliar, W. Krauth, and M. J. Rozenberg, Dynamical mean-field theory of strongly correlated fermion systems and the limit of infinite dimensions, *Rev. Mod. Phys.* 68(1), 13 (1996)
39. M. M. Boyd, T. Zelevinsky, A. D. Ludlow, S. Blatt, T. Zanon-Willette, S. M. Foreman, and J. Ye, Nuclear spin effects in optical lattice clocks, *Phys. Rev. A* 76(2), 022510 (2007)
40. G. K. Campbell, M. M. Boyd, J. W. Thomsen, M. J. Martin, S. Blatt, M. D. Swallows, T. L. Nicholson, T. Fortier, C. W. Oates, S. A. Diddams, N. D. Lemke, P. Naidon, P. Julienne, J. Ye, and A. D. Ludlow, Probing interactions between ultracold fermions, *Science* 324(5925), 360 (2009)
41. M. Dzero, K. Sun, V. Galitski, and P. Coleman, Topological Kondo insulators, *Phys. Rev. Lett.* 104(10), 106408 (2010)
42. T. Esslinger, Fermi–Hubbard physics with atoms in an optical lattice, *Annu. Rev. Condens. Matter Phys.* 1(1), 129 (2010)
43. I. Bloch, J. Dalibard, and S. Nascimbene, Quantum simulations with ultracold quantum gases, *Nat. Phys.* 8(4), 267 (2012)
44. Y. Zhong, K. Liu, Y. F. Wang, Y. Q. Wang, and H. G. Luo, Half-filled Kondo lattice on the honeycomb lattice, *Eur. Phys. J. B* 86(5), 195 (2013)
45. L. De Leo, C. Kollath, A. Georges, M. Ferrero, and O. Parcollet, Trapping and cooling fermionic atoms into Mott and Néel states, *Phys. Rev. Lett.* 101(21), 210403 (2008)
46. V. W. Scarola, L. Pollet, J. Oitmaa, and M. Troyer, Discerning incompressible and compressible phases of cold atoms in optical lattices, *Phys. Rev. Lett.* 102(13), 135302 (2009)
47. S. Chiesa, C. N. Varney, M. Rigol, and R. T. Scalettar, Magnetism and pairing of two-dimensional trapped fermions, *Phys. Rev. Lett.* 106(3), 035301 (2011)
48. T. Senthil, M. Vojta, and S. Sachdev, Weak magnetism and non-Fermi liquids near heavy-fermion critical points, *Phys. Rev. B* 69(3), 035111 (2004)

49. M. Vojta, Orbital-selective Mott transitions: Heavy fermions and beyond, *J. Low Temp. Phys.* 161(1–2), 203 (2010)

50. T. Paiva, R. Scalettar, M. Randeria, and N. Trivedi, Fermions in 2D optical lattices: Temperature and entropy scales for observing antiferromagnetism and superfluidity, *Phys. Rev. Lett.* 104(6), 066406 (2010)

51. M. Jarrell, H. Akhlaghpour, and Th. Pruschke, Periodic Anderson model in infinite dimensions, *Phys. Rev. Lett.* 70(11), 1670 (1993)

52. M. J. Rozenberg, G. Kotliar, and H. Kajueter, Transfer of spectral weight in spectroscopies of correlated electron systems, *Phys. Rev. B* 54(12), 8452 (1996)

53. C. J. Wu, J. P. Hu, and S. C. Zhang, Exact $SO(5)$ symmetry in the spin-3/2 fermionic system, *Phys. Rev. Lett.* 91(18), 186402 (2003)

54. C. J. Wu, Exotic many-body physics with large-spin Fermi gases, *Physics* 3, 92 (2010)

55. D. Wang, Y. Li, Z. Cai, Z. C. Zhou, Y. Wang, and C. J. Wu, Competing orders in the 2D half-filled $SU(2N)$ Hubbard model through the pinning-field quantum Monte Carlo simulations, *Phys. Rev. Lett.* 112(15), 156403 (2014)

56. Z. C. Zhou, D. Wang, Z. Y. Meng, Y. Wang, and C. J. Wu, Mott insulating states and quantum phase transitions of correlated $SU(2N)$ Dirac fermions, *Phys. Rev. B* 93(24), 245157 (2016)

57. S. M. Ramos, M. B. Fontes, E. N. Hering, M. A. Continentino, E. Baggio-Saitovich, F. D. Neto, E. M. Bittar, P. G. Pagliuso, E. D. Bauer, J. L. Sarrao, and J. D. Thompson, Superconducting quantum critical point in $CeCoIn_{5-x}Sn_x$, *Phys. Rev. Lett.* 105(12), 126401 (2010)

58. D. J. Scalapino, A common thread: The pairing interaction for unconventional superconductors, *Rev. Mod. Phys.* 84(4), 1383 (2012)

59. P. W. Anderson, P. A. Lee, M. Randeria, T. M. Rice, N. Trivedi, and F. C. Zhang, The physics behind high-temperature superconducting cuprates: the plain vanilla version of RVB, *J. Phys.: Condens. Matter* 16(24), R755 (2004)

60. P. A. Lee, N. Nagaosa, and X. G. Wen, Doping a Mott insulator: Physics of high-temperature superconductivity, *Rev. Mod. Phys.* 78(1), 17 (2006)

61. Y. Zhong, L. Zhang, C. Shao, and H. G. Luo, Superfluid response in heavy fermion superconductors, *Front. Phys.* 12(5), 127101 (2017)

62. M. Nakagawa and N. Kawakami, Laser-induced Kondo effect in ultracold alkaline-earth fermions, *Phys. Rev. Lett.* 115(16), 165303 (2015)